

GTP-Induced Conformational Changes in Translin: A Comparison between Human and *Drosophila* Proteins^{†,‡}

Kundan Sengupta,^{§,||} Radhika P. Kamdar,[§] Jacinta S. D'Souza,[§] Sourajit M. Mustafi,[⊥] and Basuthkar J. Rao^{*,§}

Departments of Biological Sciences and Chemical Sciences, Tata Institute of Fundamental Research, Homi Bhabha Road, Mumbai 400 005, India

Received March 24, 2005; Revised Manuscript Received October 18, 2005

ABSTRACT: Human translin is a conserved protein, unique in its ability to bind both RNA and DNA. Interestingly, GTP binding has been implicated as a regulator of RNA/DNA binding function of mouse translin (TB-RBP). We cloned and overexpressed the translin orthologue from *Drosophila melanogaster* and compared its DNA/RNA binding properties in relation to GTP effects with that of human protein. Human translin exhibits a stable octameric state and binds ssDNA/RNA/dsDNA targets, all of which get attenuated when GTP is added. Conversely, *Drosophila* translin exhibits a stable dimeric state that assembles into a suboctameric (tetramer/hexamer) form and fails to bind ssDNA and RNA targets. Interestingly enough, CD spectral analyses, partial protease digestion profile revealed GTP-specific conformational changes in human translin, whereas the same were largely missing in *Drosophila* protein. Isothermal calorimetry delineated specific heat changes associated with GTP binding in human translin, which invoked subunit “loosening” in its octamers; the same effect was absent in *Drosophila* protein. We propose that GTP acts as a specific molecular “switch” that modulates the nucleic acid binding function selectively in human translin, perhaps by affecting its octameric configuration.

Human translin is a ring-shaped octameric protein conserved across evolution and implicated in a variety of cellular functions, from chromosomal translocations to cell division (1–3). It is a rare eukaryotic protein that binds to both DNA and RNA (1, 4, 5). Testes–brain RNA binding protein (TB-RBP),¹ the mouse orthologue of human translin, binds to sequence elements that are present in the 3'-untranslated regions of mRNAs enriched in the brain and testes, thus regulating their translation (4–6). Translin also binds to consensus sequences of chromosomal break point regions associated with leukemia and lymphoma, with a high binding affinity, in the nanomolar range, to single-stranded DNA ends (1, 7, 8). It is recruited to the nucleus (i) in lymphoid cells, where double strand breaks are a prerequisite to mediate

V(D)J recombination, and (ii) in cells, where double strand breaks are induced by DNA damaging drugs such as etoposide and mitomycin C (1, 7). Translin binds to microsatellite repeats (enriched in telomeres) with high affinity and undergoes marked changes in its conformation (9, 10). Recent studies have shown that translin possesses both single-stranded and double-stranded ribonuclease activities (11). Yeast two-hybrid and other biochemical assays revealed a 33 kDa protein called TRAX (translin-associated factor X) as an interactor of translin (12, 13). TRAX binding to TB-RBP lowers its RNA binding affinity and marginally enhances its DNA binding ability (14). However, the mechanisms that are involved in mediating this selectivity of translin toward RNA or DNA by TRAX remain elusive.

Sequence analyses have shown that translin/TB-RBP has a conserved putative GTP binding motif, “VTAGD”, toward its C-terminus. However, the putative GTP binding motif of translin from *Drosophila* has a methionine in place of alanine (ref 15 and unpublished data). The sequence motif VTAGD shares homology with the DXXG/DTAGQ sequence found in low molecular mass GTP binding proteins (16–19). Nucleic acid binding studies with TB-RBP show that GTP decreases its binding affinity toward RNA by more than 50%, while the DNA binding affinity remains unaltered (20). On the basis of this observation, a novel GTP-based mechanism that modulates the nucleic acid binding affinity of TB-RBP has been suggested. Mutation at its GTP binding site led to a reduction in the binding ability of protein to RNA transcripts, implicating that the GTP binding motif may be required for RNA binding function (20). TB-RBP crystals tend to crack when soaked in a solution of GTP, indicating a role for GTP in structural alterations of TB-RBP (21).

[†] This work was supported by funds from the Tata Institute of Fundamental Research.

[‡] Nucleotide sequence data for the translin orthologue of *Drosophila melanogaster* (referred to here as *Drosophila* translin) are available in the GenBank database under the accession number AY392453.

* Corresponding author. Telephone: 091-22-22782606. Fax: 091-22-22804610. E-mail: bjr@tifr.res.in. URL: <http://www.tifr.res.in/~dbs/faculty/bjr/>.

[§] Department of Biological Sciences, Tata Institute of Fundamental Research.

^{||} Present address: National Cancer Institute, National Institutes of Health, Bethesda, MD.

[⊥] Department of Chemical Sciences, Tata Institute of Fundamental Research.

¹ Abbreviations: TB-RBP, testes–brain RNA binding protein; GTP, guanosine triphosphate; GDP, guanosine diphosphate; dGTP, deoxyguanosine triphosphate; Gpp(NH)p, guanosine 5'-(β , γ -imido)triphosphate; ATP, adenosine triphosphate; HRP, horseradish peroxidase; CD, circular dichroism; MALDI-TOF, matrix-assisted laser desorption ionization time of flight; ITC, isothermal calorimetry; FPLC, fast protein liquid chromatography; ssDNA, single-stranded DNA; dsDNA, double-stranded DNA.

Transfection studies in mammalian cell lines, with wild-type TB-RBP, exhibit a normal distribution of translin in the cytoplasm and nuclei, whereas transfection with a form that is mutated in the GTP binding motif leads to a punctate pattern of protein distribution and eventually to cellular apoptosis (20). The in vivo mechanisms that mediate transitions in translin oligomerization upon GTP binding remain to be analyzed.

In the current study, we delineate GTP-specific conformational changes in human translin, which appear to be largely missing in the translin orthologue from *Drosophila*, the protein that we cloned and overexpressed for the first time [GenBank accession number AY392453 (ref 15 and unpublished data)]. Binding studies revealed that human translin is proficient in binding ssDNA/RNA/dsDNA targets, whereas its orthologous protein from *Drosophila* fails to bind ssDNA and RNA. Interestingly enough, addition of GTP seems to attenuate nucleic acid binding function of human translin, leading to reduced binding to the ssDNA/RNA/dsDNA targets tested here.

MATERIALS AND METHODS

Materials. Nucleotides, anti-histidine antibody, secondary anti-mouse-HRP, and the enhanced chemiluminescence kit (ECL) were obtained from Amersham Biosciences, while restriction enzymes, trypsin, and enhanced DAB reagent were from Roche. Anti-rat HRP was obtained from Santacruz Biotechnologies. Human translin (N-terminal histidine-tagged clone) was obtained as a kind gift from Dr. M. Kasai, National Institute of Health, Japan, from where the overexpressed translin was purified using standard methods (1, 8). The translin orthologue from *Drosophila melanogaster* (or *Drosophila* translin) was cloned, expressed, and purified. (A partial sequence of translin from *D. melanogaster* has been deposited in GenBank, accession number AY392453; <http://flybase.bio.indiana.edu> and ref 15 and unpublished data.) *Prm2* RNA oligonucleotide was obtained from Dharmacon. ssDNA oligonucleotides were obtained from DNA Technology (Denmark). Yeast-soluble RNA enriched in tyrosine and valine tRNA fractions (type III, Sigma) was used as a general RNA strand.

Circular Dichroism Spectroscopy (CD Spectroscopy). The CD measurements for translin/*Drosophila* translin were carried out in a JASCO-600 CD spectropolarimeter. The CD scans were recorded within the wavelength range of 200–270 nm, and ellipticity values were recorded at 222 nm at sensitivity set to 20 mdeg and scan speed 20 nm/min with step size of 0.2 nm (Figure 2), the time constant being set to 0.5 s. The measurements were carried out in a cuvette of 1 mm path length, in a reaction volume of 800 μ L, in 1 \times translin buffer [10 mM Tris-HCl (pH 7.5), 50 mM NaCl, 10 mM EDTA, and 4% glycerol]. In the reaction mixture containing translin (final concentration \sim 2.0 μ M octamer), individual titrations were performed with NTPs [NTP = GTP, dGTP, Gpp(NH)_p, ATP] to achieve a concentration range of 2.0–32.0 μ M (Figure 2B). The reaction mixture was incubated for 5 min at 25 $^{\circ}$ C. The CD spectra were recorded twice for each concentration and corrected for background fluctuations by scanning only the buffer between 200 and 270 nm prior to the actual CD recordings with translin. Similar scans were also recorded for *Drosophila* translin (final concentration \sim 2.0 μ M) (Figure 2C).

Table 1: Molecular Mass of Cleavage Products Obtained on MALDI-TOF Analysis of the Trypsin Time Course of Translin (A) and *Drosophila* Translin (B) and Possible Cleavage Residue Obtained from a Theoretical Tryptic Digest of Translin^a

molecular mass of fragment (Da)	possible cleavage residue
(A) Translin	
25620	lysine 219
\sim 15701–15705	arginine 153
\sim 12677–670	arginine 129
\sim 8123–8134	arginine 182
\sim 5709–5805	lysine 192
\sim 2184–3380	lysine 215 or 219
(B) <i>Drosophila</i> Translin	
\sim 25339	lysine 216
\sim 19246	arginine 167
\sim 18839	arginine 154
\sim 16616	lysine 127
\sim 5627.3	arginine 193

^a From <http://us.expasy.org/tools/peptidecutter/>.

Limited Proteolysis by Trypsin and Matrix-Assisted Laser Desorption Ionization Time-of-Flight (MALDI-TOF) Analysis. Limited proteolysis was performed by incubating translin/*Drosophila* translin (480 μ g/mL) with trypsin (10 μ g/mL) in an assay buffer (10 mM Tris-HCl, pH 7.5, 50 mM NaCl, and 4% glycerol) at room temperature. Aliquots withdrawn at specific time points from the reaction mixture were quenched in a 5 \times sample buffer [20 mM EDTA, 50 mM Tris-HCl (pH 6.8), 2% SDS, 5 mM DTT, 0.1% Bromophenol blue, and 10% glycerol], boiled immediately to inactivate the trypsin, and resolved on a 15% SDS–PAGE, followed either by silver staining (data not shown) or by western blotting using anti-histidine antibody (Figure 3A,B). For monitoring GTP-mediated effects, translin/*Drosophila* translin was preincubated with 100 μ M GTP for 10 min (in separate reactions) and further subjected to limited proteolysis with trypsin for 0–5 min, respectively. For MALDI-TOF, reaction mixtures were quenched at intervals of 2, 5, and 10 min, respectively, in 1 μ L of trifluoroacetic acid (pH 5.6) and mixed with sinnappinic acid matrix. These mixtures were spotted on a target MALDI plate, allowed to dry at room temperature, and analyzed by the MASSLYNX program (data not shown) (summarized in Table 1).

Isothermal Calorimetry (ITC) Analyses. Isothermal calorimetric measurements were performed with a Microcal Omega titration calorimeter (22, 23). Samples were centrifuged and degassed prior to titration and examined for precipitation after titration. Titration of GTP against human translin consisted of injecting 5 μ L aliquots of GTP (1.575 mM) into 0.056 mM protein solution every 3 min to ensure that the titration peak returned to baseline prior to the next injection. A total of 25 injections were carried out. Similarly, titration of GTP against *Drosophila* translin consisted of injecting 4 μ L aliquots of GTP (1.05 mM) into the protein solution (0.0588 mM) every 3 min. A total of 70 injections were carried out in order to confirm the trend in the range where the GTP:protein ratio was higher than 1:1. Aliquots of the nucleotide solution (same concentrations) were injected into 1 \times phosphate-buffered saline (pH = 7.4) (without protein) in an independent ITC experiment to subtract the heat of dilution (Figure 4). All experiments were repeated at least twice.

Gel Electrophoresis (Native Polyacrylamide) and Fast Performance Liquid Chromatography (FPLC). Purified



FIGURE 1: Protein sequence alignment of human translin and *Drosophila* translin. Identical residues between the two proteins are boxed. The consensus residues are derived from the multiple alignments between several known translin orthologues. The regions of conservation encompass (I and II) the RNA and DNA binding motif, (III) the putative GTP binding motif, and (IV) the conserved C-terminal region.

protein samples of human translin and *Drosophila* translin (~10 μ g) were suspended in a buffer containing 10 mM Tris-HCl (pH 7.5), 50 mM NaCl, 5 mM EDTA, and 5% glycerol in a final volume of 20 μ L, resolved on a 6% native PAGE, and run at a constant voltage of 50 V for 10 h. The gel was visualized by silver staining (Figure 5A). FPLC studies were performed on a Hi-Load 75 FPLC column on an AKTA-FPLC machine. The FPLC column was equilibrated using 1 \times phosphate-buffered saline of pH 7.4. Separate FPLC runs were performed with translin (~0.2 mg/mL) and *Drosophila* translin (~0.3 mg/mL) and continued to a total column volume of 100 mL at a flow rate of 1.0 mL/min. The absorbance was measured at 280 nm in a cell of 5 mm path length (Figure 5B).

DNA Labeling, Electrophoretic Mobility Shift, and Linear Duplex DNA End Binding Assay. Labeled ssDNA gel-shift analyses were done using various length oligonucleotides as described earlier (8) (Figure 6C). Unlabeled ssDNA gel shifts were done using a 121-mer long oligonucleotide (8) (Figures 6A and 7C). A 2.9 kb cloning vector pGEM7Z (35 μ g) was partially digested with the restriction enzyme *Nsi*I (5 units) in a 25 μ L reaction volume for 1 h at 37 $^{\circ}$ C in the appropriate digestion buffer. The reaction was quenched at 65 $^{\circ}$ C for 15 min. The partially cut plasmid DNA was incubated in DNA binding buffer with 100 μ M GTP, and this reaction mixture was further incubated with translin at the indicated concentrations at room temperature for a duration of 20 min followed by electrophoresis on a 0.8% agarose gel at 50 V for 6 h at 18 $^{\circ}$ C and stained with ethidium bromide (0.5 μ g/mL) for 10 min (Figure 7A).

pGEM7Z (25 μ g/mL) cloning vector as described in the above assay was double digested using *Dra*I and *Pvu*II enzymes (10 units) in a 40 μ L reaction volume (2.5 μ g in 40 μ L for 1 h at 37 $^{\circ}$ C) with the appropriate buffer. The reaction was quenched as described above. The digested plasmid was incubated with 100 μ M GTP and translin at the required concentrations for 20 min. The reaction mixture was then resolved by agarose gel electrophoresis (0.8%) at 50 V for 6 h at 18 $^{\circ}$ C and stained with ethidium bromide (0.5 μ g/mL) for 10 min (Figure 7B).

RNA Gel-Shift Assay. Yeast-soluble RNA enriched in tyrosine and valine tRNA fractions (type III, Sigma) was incubated with increasing concentrations of translin (0, 2,

5, 10, 20 μ M) and 500 μ M GTP at 4 $^{\circ}$ C for 1 h and then resolved on a 6% native PAGE and stained with ethidium bromide. The same assay was also performed with *Prm*2 oligonucleotide (39-mer) (24) with increasing concentrations of translin (0, 2, 3, 4, 6, and 8 μ M) and 500 μ M GTP and dGTP (Figure 7D).

RESULTS

In this study, we have used biochemical and biophysical assays to analyze the effect of GTP on human and *Drosophila* translin proteins. We cloned, overexpressed, and purified the translin orthologue from the fruitfly *D. melanogaster* (ref 15 and unpublished data). The sequence of the cloned gene is identical with the annotated gene in the flybase and shows 52% identity and 67% similarity with the amino acid sequence of human translin (Figure 1). Here, we used *Drosophila* translin for comparison as a natural variant of human translin: among other sequence changes, alanine is replaced by methionine in the GTP binding motif VTAGD of *Drosophila* protein (Figure 1). The biochemical comparison between the two proteins might unveil the basis of their specialized biological functions, if any.

Effect of GTP on Translin Secondary Structure and Comparison with *Drosophila* Translin: CD Spectroscopy. Crystal structure analyses showed that translin/TB-RBP is a highly structured oligomeric protein where the monomer is composed of about 70% α -helices, 25% random coils, and 5% β -sheets (21, 25). To study if GTP has any effect on the secondary structure of translin, we performed CD spectroscopy. CD spectra of translin (2.0 μ M octamer) recorded between 200 and 270 nm showed an ellipticity of -15.0 mdeg at 222 nm, revealing high α -helical content (21, 25) (Figure 2A). Upon GTP titration, a marked decrease in the negative ellipticity (from $\theta = -15.0$ mdeg to $\theta = -2.0$ mdeg) was observed that saturated by 30 μ M nucleotide concentration (Figure 2A,B). To test the specificity of GTP effect, translin was titrated with GDP, ATP, Gpp(NH)p, or dGTP followed by ellipticity measurements (Figure 2B). GDP titration showed a lesser decline in ellipticity, which saturated at lower nucleotide concentration (~8 μ M) (Figure 2B). In comparison, other nucleotides [ATP, dGTP, and the poorly hydrolyzable analogue of GTP, i.e., Gpp(NH)p] showed a much smaller decrease in ellipticity where the

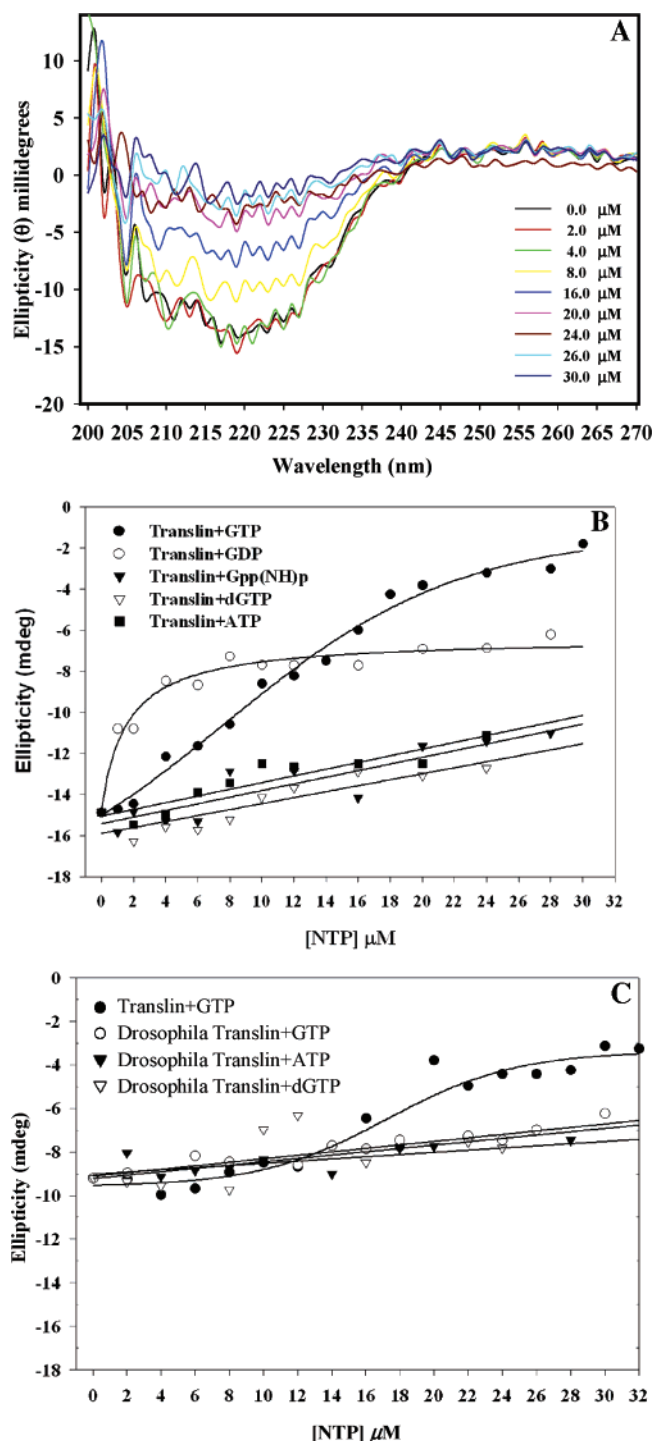


FIGURE 2: Effect of GTP and related nucleotides on protein conformation by CD spectral analysis. (A) Representative CD scans showing the effect of GTP on translin secondary structure. CD scans were performed on translin ($\sim 2.0 \mu\text{M}$ octamer) in the absence or presence of increasing concentrations of GTP. Colored symbols in the graph legend indicate the GTP concentration used for each titration. (B) Effect of GTP and other nucleotides on the CD spectral profile of translin. Average ellipticity values of translin at 222 nm (from panel A) of three independent CD scans were plotted (Y-axis) against [NTP] (μM) (X-axis). Translin (final concentration $2 \mu\text{M}$) was titrated with the following nucleotides, GTP, GDP, Gpp(NH)p, dGTP, and ATP, within a concentration range of $2\text{--}32 \mu\text{M}$ in independent experiments. (C) CD spectral analysis was performed on *Drosophila* translin ($\sim 2.0 \mu\text{M}$) which was independently titrated with GTP, ATP, and dGTP, while translin ($\sim 2.0 \mu\text{M}$) was used as a positive control and was titrated with GTP at the indicated concentration range. Ellipticity (in millidegrees), recorded at 222 nm, was plotted (Y-axis) against NTP concentration (X-axis).

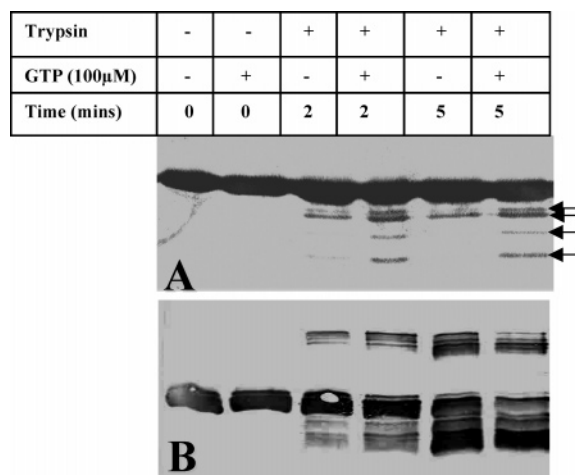


FIGURE 3: Effect of GTP on partial proteolysis of human and *Drosophila* translins. Limited proteolysis was performed on (A) translin ($480 \mu\text{g/mL}$) and (B) *Drosophila* translin ($560 \mu\text{g/mL}$) with trypsin ($10 \mu\text{g/mL}$) at a time course of 0, 2, and 5 min in the presence of $100 \mu\text{M}$ GTP. The reaction was quenched at the indicated time points and resolved on a 15% SDS-PAGE gel. Western analysis was done using anti-histidine antibody. Enhanced fragmentations due to GTP additions resulting from cleavages at the C-terminal domain are indicated in black arrows.

responses, unlike that of ATP/ADP, were of a nonsaturating type, suggesting the underlying nonspecificity in these nucleotide effects (Figure 2B). Interestingly, *Drosophila* translin, like human translin, also showed a high negative ellipticity at $\sim 222 \text{ nm}$, reflecting high α -helical content in the structure (Figure 2C). However, upon titration with GTP, *Drosophila* translin showed hardly any decline in the negative ellipticity with either GTP or other analogues (ATP or dGTP) ($2.0\text{--}32.0 \mu\text{M}$) (Figure 2C). In fact, GTP response was similar to that of other nucleotide analogues, suggesting that no specific changes of the type induced in human protein were discernible in *Drosophila* protein by GTP. As expected, in the same set, human translin control exhibited a discernible change with GTP.

GTP-Induced Changes Lead to Enhanced Accessibility of the C-Terminal Domain to Protease Action: Comparison of Translin with *Drosophila* Protein. A limited trypsin proteolysis experiment was done to biochemically assess conformational changes in translin and *Drosophila* protein. The trypsin time course followed by immunoblotting of separated cleavage products using an anti-N-terminal histidine tag antibody revealed enhanced cleavages at the C-terminal end of the proteins. Such enhanced C-terminal cleavages were observed only in the presence of GTP ($100 \mu\text{M}$) specifically with translin (Figure 3A) and not with *Drosophila* protein (Figure 3B). This result suggested that GTP-mediated changes were specific to translin and was in line with CD changes observed in the previous experiment. MALDI-TOF analyses of the total tryptic digestion profile revealed that both proteins liberated proteolyzed fragments that predominantly belonged to $24\text{--}27$ and $6\text{--}8 \text{ kDa}$ size categories where the former primarily originated from C-terminal cleavages (Table 1). GTP addition seems to further enhance these C-terminal cleavages specifically in translin.

Isothermal Calorimetry Studies of GTP Binding to Translin/*Drosophila* Translin Proteins. We performed isothermal calorimetry (ITC) to probe heat changes associated with

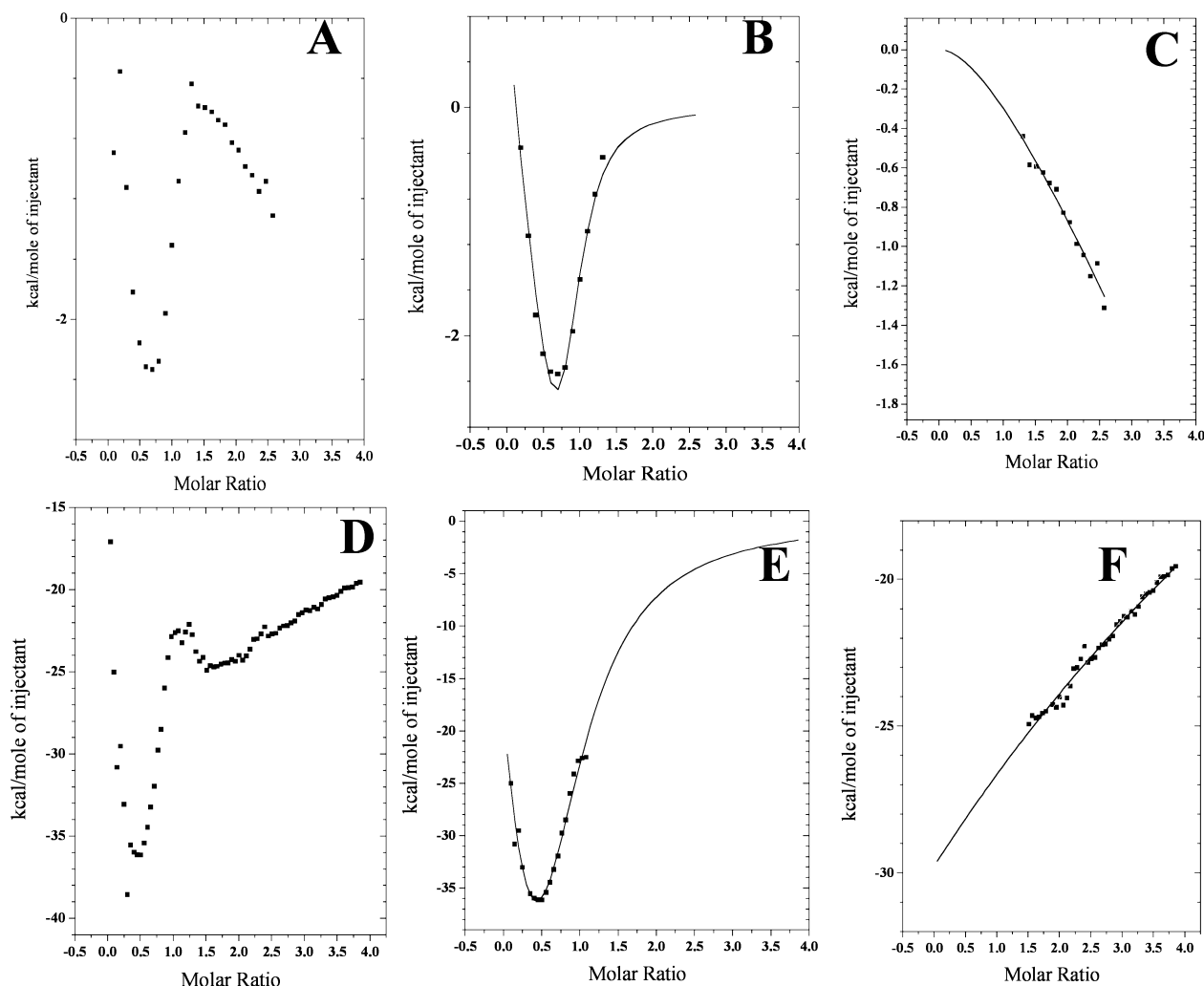


FIGURE 4: Isothermal calorimetric analyses of human and *Drosophila* translins: effect of GTP. (A) Titration curve of 1.575 mM GTP against 56.0 μ M translin after subtraction of heat of dilution (see Materials and Methods). Heat changes were plotted against the molar ratio of GTP:translin monomer (22, 23). (B) The titration curve obtained up to a molar ratio of $\sim 1:1$ was best fitted to a model involving two independent sets of sites. (C) The titration curve beyond the molar ratio of $\sim 1:1$ was best fitted independently to a dissociation model. (D) Titration curve of 1.05 mM GTP against 58.8 μ M *Drosophila* translin after subtraction of heat of dilution (see Materials and Methods). Heat changes were plotted against the molar ratio of GTP:*Drosophila* translin monomer. (E) The titration curve obtained up to a molar ratio of $\sim 1:1$ was best fitted to a model involving two independent sets of sites. (F) The titration curve beyond the molar ratio of $\sim 1:1$ was best fitted independently to a model involving a single nonspecific site.

GTP-mediated effects in translin and *Drosophila* protein. A fixed amount of protein was titrated with GTP. The recovered heat changes are plotted as a function of increasing GTP:protein monomer ratios (Figure 4A,D). Two distinct phases of heat changes were observed with either protein. In the first phase, as the GTP:protein monomer ratio increased from 0:1 to 1:1, the initial curve showed an exothermic followed by an endothermic change. Nearly similar best curve fits were obtained for both proteins in this titration range (compare panels B and E of Figure 4). However, in the final phase of titration, as the ratio increased beyond 1:1, the heat changes observed with translin were markedly different from *Drosophila* protein (Figure 4A,D). In this high GTP range, translin showed an exponential decrease in enthalpy, whereas *Drosophila* protein showed a monotonic rise in enthalpy. This difference was evident in the best curve fits retrieved from the data (compare panels C and F of Figure 4).

The data of the first part of the titration curve (where the ratio increases from 0:1 to 1:1) obtained from translin were fitted to two sets of binding sites with $N_1 = 0.415$ and $N_2 =$

0.415, taking into account the monomeric concentration of protein (22, 23). The N_1 type of binding is exothermic in nature whereas N_2 is endothermic (Table 2A), both associated with similar binding affinity in the micromolar range (K_1 and K_2 in Table 2A). Since these two sets of sites are best fitted to an independent-site model, their binding patterns cannot be correlated as either parallel or sequential. As the GTP:protein ratio increases beyond 1:1, the model hypothesizes that occupancy of the putative final site with GTP induces dissociative change within the translin octamer, as evidenced by the exponential decrease in the enthalpy curve in the second stage of titration (Figure 4C). This part was fitted independently to a dissociation model (Table 2B). The fit was found to be stable. The dissociation constant was in the millimolar range (K in Table 2B). Interestingly, under similar conditions, the heat changes recovered from GTP titration with *Drosophila* protein were similar to that of human translin in the first part and different in the second part (Figure 4D). As with translin, the data of *Drosophila* protein from the first part of the titration curve (where the

Table 2: ITC Results for Titration of GTP against Translin and *Drosophila* Translin

(A) Specific Binding Pattern of Translin			
binding constant for human translin (M ⁻¹)	Gibbs free energy ΔG (kJ/mol)	enthalpy ΔH (kJ/mol)	entropy TΔS (kJ/mol)
K ₁ = 4.86 × 10 ⁵	-32.44	69.34 ± 3.29	101.88
K ₂ = 3.47 × 10 ⁵	-31.61	-91.43 ± 5.8	-59.6
(B) Dissociation Pattern of Translin			
dissociation constant for human translin (M ⁻¹)	enthalpy ΔH (kJ/mol)		
K = 4.66	7.24 ± 0.1		
(C) Specific Binding Pattern of <i>Drosophila</i> Translin			
binding constant for <i>Drosophila</i> translin (M ⁻¹)	Gibbs free energy ΔG (kJ/mol)	enthalpy ΔH (kJ/mol)	entropy TΔS (kJ/mol)
K ₁ = 5.84 × 10 ⁴	-27.19	-1.744 × 10 ³	-1.714 × 10 ³
K ₂ = 8.32 × 10 ⁴	-28.07	1.027 × 10 ³	1.055 × 10 ³
(D) Nonspecific Binding of <i>Drosophila</i> Translin			
nonspecific binding constant for <i>Drosophila</i> translin (M ⁻¹)	enthalpy ΔH (kJ/mol)		
K = 8.17	-26.69 × 10 ³		

ratio increases from 0:1 to 1:1 (Figure 4D) could be best fitted to two independent, noncooperative binding site models with $N_1 = 0.344$ and $N_2 = 0.344$ (Figure 4E). Out of N_1 and N_2 binding, one was exothermic and the other endothermic in nature, both being in $\sim 100 (\mu M)^{-1}$ of binding affinity (K_1 and K_2 in Table 2C). Since the two sets of sites are independent of each other, their binding pattern cannot be correlated as either parallel or sequential. It is important to reiterate that as the GTP:protein ratio was increased beyond 1:1, the heat changes recovered from the *Drosophila* protein system were markedly different from that of human translin (compare panels D and F with panels A and C of Figure 4, respectively). As per the model, it appears that, following near saturation of GTP sites, incoming excess GTP leads to low-affinity, nonspecific binding to *Drosophila* protein (K in Table 2D), reflecting monotonic heat changes (Figure 4F). Taken together, these results suggest a model where GTP binding seems to induce a dissociative change between subunits of the human translin octamer, whereas the same effect is not observed in *Drosophila* translin.

Oligomerization Status: Human versus *Drosophila* Translin. Native gel assay showed that *Drosophila* translin migrated distinctly faster, as one band compared to that of human protein, showing a ladder of multiple forms (Figure 5A). On the basis of a host of earlier studies (8, 26, 27), one can infer that the multiple forms associated with human translin reflect its octameric and higher octameric forms of protein. The gel assay result seems to suggest that *Drosophila* protein assembles into a somewhat unique, but smaller oligomeric form than that of octameric human translin. To estimate the native molecular mass of *Drosophila* translin, gel filtration by FPLC was performed along with standard molecular mass markers. Translin eluted as a stable octamer, while *Drosophila* protein migrated as a dimer (Figure 5B).

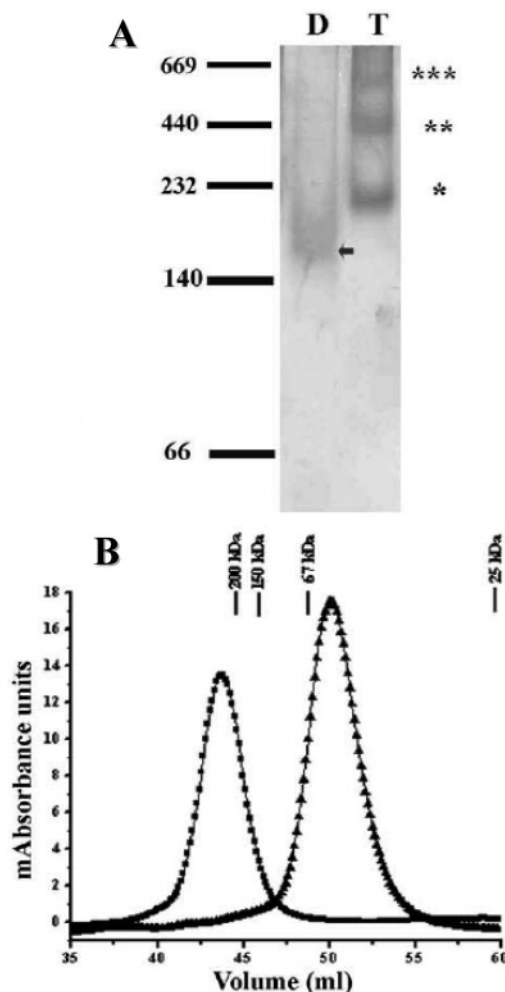


FIGURE 5: Comparison of *Drosophila* and human translins under native conditions. (A) Native gel analysis. *Drosophila* translin (D) and human translin (T) (both $\sim 10 \mu g$) were resolved on a 5% native gel and visualized by silver staining. Molecular mass marker positions are indicated alongside the gel. *Drosophila* translin oligomeric state (arrow). Translin: *, octamer; **, double octamer; ***, higher oligomers. (B) FPLC analysis under native conditions. FPLC elution profiles of translin (filled square) and *Drosophila* translin (filled triangle) were analyzed in separate elutions. Molecular mass standards were also run under the same FPLC conditions whose peak elution positions are indicated.

Both analyses, put together, seem to suggest that *Drosophila* translin protein perhaps exists as an oligomer that is smaller than octamer (tetramer/hexamer), which under conditions of gel filtration dissociates into stable dimers. On the contrary, human translin exists as a stable octamer even under the dissociating conditions of gel filtration and also exhibits the propensity of aggregating further into higher octamers, which is absent in *Drosophila* protein.

ssDNA and RNA Binding Ability of Human and *Drosophila* Translin. We tested whether *Drosophila* translin exhibits as good binding ability as human translin toward ssDNA and RNA. The nucleic acid strands chosen were not the bona fide specific target sequences of human translin protein (20, 27) but rather general sequences that can compare the intrinsic binding ability of these two proteins in a sequence-independent manner. The ssDNA target was a 121-mer oligonucleotide strand shown earlier as a good binder of translin (8). Purified yeast-soluble RNA enriched in tyrosine and valine tRNA fractions (27) was used as general RNA

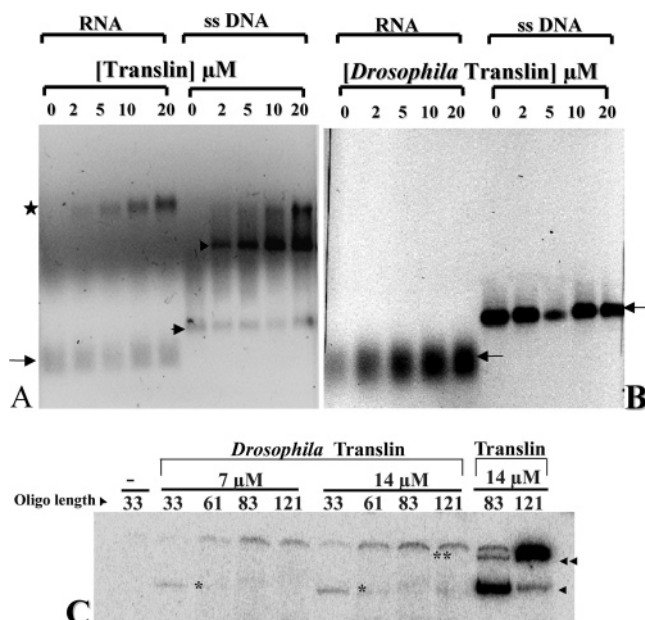


FIGURE 6: ssDNA/RNA binding analyses of human and *Drosophila* translins by gel-shift assay. (A, B) Comparison of ssDNA and RNA binding ability of human and *Drosophila* translin. An agarose gel electrophoresis was performed with (A) translin and (B) *Drosophila* translin within a protein concentration range of 0.0–20.0 μM with yeast-soluble RNA enriched in tyrosine and valine tRNA fractions (357 μM) and ssDNA (357 μM), respectively. Symbols: (A) star, RNA–translin gel-shifted complex; arrow, free RNA; arrowhead, translin–ssDNA gel-shifted complex; short arrow, free ssDNA. (B) Arrows indicate unbound RNA and ssDNA, respectively. (C) A native gel-shift assay was performed with *Drosophila* translin (7.0 and 14.0 μM, respectively) with the indicated ssDNA substrates labeled with [γ - 32 P]ATP (8). The lengths of ssDNA substrates used are indicated. Translin was used as a comparative positive control. The gel-shift complex (*) and supershifted complex (**) are indicated for *Drosophila* translin. Single and double arrowheads indicate translin gel-shifted and supershifted complexes, respectively. Only the top portion of the gel containing gel-shifted complexes has been shown, and the free duplex is not shown. The input radioactivity was same in all of the lanes.

strands for binding assays. Gel-shift analyses as a function of protein concentration revealed that human translin binding led to gel-shifted complexes with both ssDNA as well as RNA targets (Figure 6A). On the contrary, *Drosophila* protein did not show any detectable gel-shifted complexes with either ssDNA or RNA targets (Figure 6B), suggesting lack of protein binding. As shown by us earlier (8), we verified whether even in the current assay conditions human translin exhibits ssDNA length-dependent gel shifting. As expected, human translin yielded gel-shifted complexes where the longer target facilitated a relatively larger ssDNA–protein complex (indicated by the double arrowhead in Figure 6C) as compared to the shorter target complex (indicated by the single arrowhead in Figure 6C). In comparison, *Drosophila* translin yielded very poor gel-shifted complexes whose size (as in human translin) increased with the length of the DNA target (Figure 6C). This gel assay reiterated that the ssDNA binding ability of *Drosophila* protein is rather limited, which could be barely detected even in the highly sensitive radioactive gel assay. We had noted in the earlier experiment that its binding signal was too low to be detected in the ethidium bromide staining method (Figure 6B).

GTP Leads to Attenuation in General Nucleic Acid (dsDNA, ssDNA, and RNA) Binding Ability of Human

Translin. All the following assays were performed only with human translin since *Drosophila* protein exhibited almost no binding toward both ssDNA and RNA targets (Figure 6B). In the experiments below, we tested the effect of GTP on human translin binding to dsDNA, ssDNA, and RNA.

(A) *dsDNA End-Binding Assay*. DNA binding assay was performed with a fixed amount of partially digested plasmid DNA that contained nicked, linear, and supercoiled forms of duplex DNA (Figure 7A). The DNA mixture was incubated with increasing concentrations of protein, at a fixed GTP concentration (100 μM), followed by agarose gel electrophoresis. In this gel assay, free plasmid DNA does not clearly separate from the gel-shifted complex due to its high molecular mass. Protein binding was observed as a smearing of the linear DNA species as a function of translin concentration (indicated by arrows in Figure 7A). In the same lanes, the nicked circular form showed no such smearing (indicated by arrowheads in Figure 7A). In the same assay conditions, addition of GTP seems to lower protein binding to linear DNA where no dsDNA retardation was observed (Figure 7A). To achieve better separation of gel-shifted complexes from naked dsDNA, we repeated the same experiment with shorter duplex fragments, generated by double digesting the same plasmid (used in the earlier experiment) with restriction enzymes that yield three shorter linear duplexes (800, 400, and 200 bp). Gel retardation assay revealed faint, yet distinctly well-separated gel-shifted complexes as a function of translin concentration (indicated by arrows in Figure 7B). However, in the presence of GTP (100 μM), the level of gel-shifted complexes was lowered (Figure 7B).

(B) *ssDNA Binding*. The same 121-mer ssDNA used in the earlier experiment (Figure 6A) was tested for translin binding in the presence of GTP. Protein titration revealed formation of distinct gel-shifted complexes in the absence of GTP (indicated by the asterisk in Figure 7C), the level of which reduced when GTP was present (indicated by the arrow in Figure 7C).

(C) *RNA Binding*. It is well-known that translin/TB-RBP shows high binding affinity to RNA targets enriched in the brain and the testes, respectively (4, 6). To test the effect of GTP on translin binding to RNA, we used both a nontarget general RNA strand (yeast-soluble RNA enriched in tyrosine and valine tRNA fractions used in an earlier experiment; Figure 6A) and a defined RNA target of human translin, namely, the *Prm2* sequence (24). We observed protein concentration dependent formation of gel-shifted complexes with the general RNA as well as the *Prm2* strand (Figure 7D, I and II). Both complexes essentially migrated similarly, perhaps reflecting similar size properties. Interestingly enough, the level of gel-shifted complexes formed by the general RNA strand as well as *Prm2* strand was reduced when GTP was present (Figure 7D, I and II). The GTP-mediated reduction in protein binding appeared more striking in the case of the *Prm2* strand. To test whether the GTP effect was specific or not, we repeated the same in the presence of dGTP, which revealed that the level of gel shifting in the dGTP set was similar to the control where no nucleotide was present (Figure 7D, III). This experiment suggested that GTP-mediated attenuation of *Prm2* binding was specific as the same was not observed with dGTP.

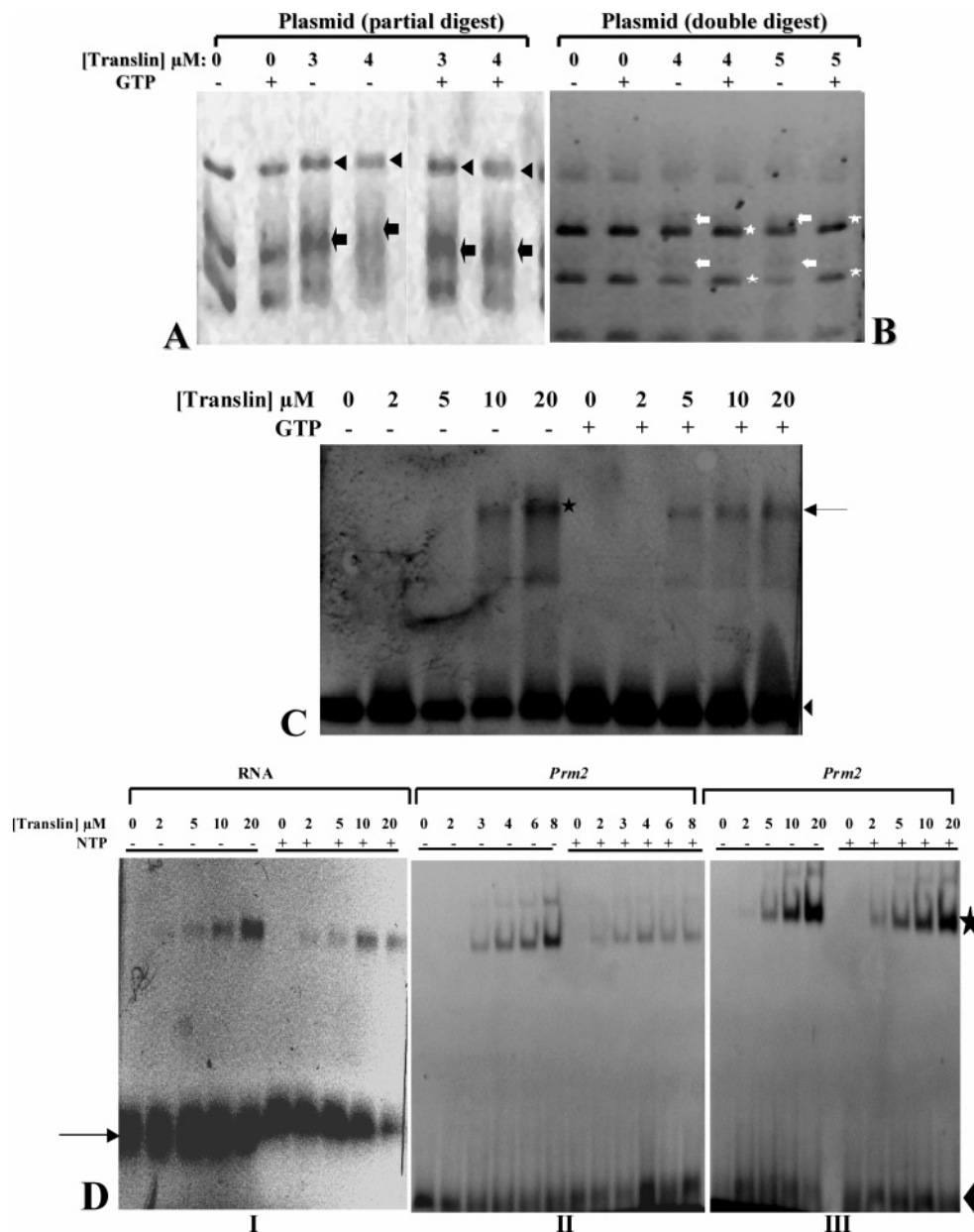


FIGURE 7: GTP lowers the DNA/RNA binding ability of human translin. (A) A partial digest of a plasmid (500 μM) was incubated with a fixed concentration of GTP and with increasing levels of translin as indicated. The reaction samples were resolved on a 0.8% agarose gel and stained with ethidium bromide. The three bands from top to bottom correspond to the nicked duplex (black triangle), linear duplex (black arrow), and supercoiled duplex, respectively. The retardation of the linear duplex is indicated by the black arrow positions. (B) A similar assay as in (A) was performed with the *DraI* and *PvuII* double digest of the same plasmid. Key: white arrow, gel-shifted complex; white star, linear DNA in the presence of GTP. (C) Effect of GTP on the ssDNA binding ability of translin. Native agarose gel electrophoresis was performed with translin (at the indicated protein concentrations) and 121-mer ssDNA (357 μM) in the absence and presence of GTP. Key: star, gel-shifted complex in the absence of GTP; arrow, gel-shifted complex in the presence of GTP; arrowhead, free 121-mer ssDNA. (D) Native gel electrophoresis performed with translin and RNA targets (357 μM) in the presence and absence of GTP: (I) yeast-soluble RNA enriched in tyrosine and valine tRNA fractions; (II) *Prm2* RNA oligonucleotide in the presence and absence of GTP; (III) *Prm2* oligonucleotide in the presence and absence of dGTP. Key: star, gel-shifted complex; arrow and arrowhead, free RNA.

DISCUSSION

Translin/TB-RBP: A Unique Oligomeric System. The translin/TB-RBP family of proteins is perhaps one of the best examples of evolutionarily conserved protein sequences with diverse oligomeric forms. Electron microscopy, gel filtration, and centrifugation studies have shown that human, mouse, *Xenopus*, and *Schizosaccharomyces pombe* translin exist as octamers/tetramers in the native state whereas chicken translin forms decamers (8, 26, 29, 30). Crystal structure analysis suggests that multimerization of translin

is achieved mainly by nondirectional hydrophobic interactions rather than directional hydrogen bonds between subunits, which facilitates an easier dynamic rearrangement of subunits in the oligomer (25).

GTP as a "Switch": A Model. Two important aspects of translin structure, relevant to function, are (i) the location of putative binding sites of RNA/DNA in the concave surface of the ellipsoidal ring and (ii) the GTP binding site at the C-terminal end (23). It is likely that translin can be "switched on" toward either RNA or DNA pathways by regulators such as GTP or TRAX depending on the signals perceived by

the cell (13, 14, 20). Studies have shown that GTP binding to TB-RBP decreases RNA binding by about 50% while DNA binding remains unaltered (20). TB-RBP crystals crack when soaked in a solution of GTP (21). A dominant negative mutation in the GTP binding motif of TB-RBP leads to cell death, implying that functions of this protein critically depend on GTP binding and other protein–protein interactions (20). Structural studies and sequence analyses of GTPases show conserved switch-like motifs G-1 to G-5, which are critical in GTP/GDP exchange, GTP-induced conformational change, and GTP hydrolysis (16–19). Closer comparison of translin shows that it shares homology with G-3 and G-4 switch regions conserved in most GTPases. The putative GTP binding site is located strategically in the translin protein oligomer (residues 159–163 between helices 5 and 6), where the C-terminal helices 5, 6, and 7 merge into a bundle, strongly interacting within the four subunits of a tetramer. These helices bundle into a “pony-tail” configuration, marking the tip of the pseudo-4-fold axis of the tetramer structure (25). We hypothesize that GTP binding and the resultant changes can significantly affect the properties of the protein oligomer via the pony-tail configuration, thereby acting as a “regulatory switch” in the protein assembly.

GTP-Mediated Conformational Changes. In the current study, we report specific GTP-mediated changes in the conformation of native human translin and compare the same with the translin orthologue from *D. melanogaster*, which shares 52% identity and 67% similarity with human translin (Figure 1). The conservation encompasses (a) the nucleic acid binding site, (b) the GTP binding site, VTMGD, with a single amino acid change where alanine in human translin is replaced by methionine, and (c) the C-terminal hydrophobic region (Figure 1). All of the approaches employed, namely, CD (Figure 2), partial protease digestion studies (Figure 3), and ITC (Figure 4), revealed that human translin undergoes striking structural changes by the action of GTP. The changes might encompass conformational alterations in the protein monomer itself and/or the way monomers assemble into oligomers. Interestingly, none of these changes were observed with *Drosophila* protein following GTP addition (Figures 2C, 3B, and 4F). ITC results seem to suggest that GTP binding affinity of *Drosophila* protein was an order of magnitude lower than that of human translin (compare K_1 and K_2 in Table 2A with those in Table 2C). Translin titration with GTP shows an exothermic followed by an endothermic change (Figure 4A,B). Data analyses also suggest that, in the best fit model, N_1 binding in translin is entropy driven (101.88 kJ/mol) and is much larger (32%) than the enthalpy contribution (69.34 ± 3.29 kJ/mol, Table 2A), reflecting that GTP binding perturbs the strong hydrophobic interactions of the C-terminal interactions in translin tetramer cups. Analogously, it has been reported that ligand binding to calcium binding proteins exposes its hydrophobic core, which leads to a significant increase in the entropy of the protein (23). It is likely that a cumulative occupancy of GTP sites leads to a sufficient strain in the translin octamer, thereby resulting in a dissociative effect between the subunits following the occupancy of the last site by GTP (Figure 4C). On the basis of ITC data, we conjecture that in *Drosophila* translin, following saturation (beyond 1:1 of GTP:protein, Figure 4D), additional GTP molecules bind nonspecifically,

without leading to any substantial structural changes (Figure 4F).

Nucleic Acid Binding Vis-à-Vis Protein Oligomeric Status and GTP-Mediated Changes. The TB-RBP/translin crystal structure data show that the DNA/RNA binding surface encompasses the concave part of the tetramer cup as a belt whose conformation critically depends on the state of the protein oligomer (21, 25). It is interesting to envisage that the ellipsoidal ring structure is critical for capturing not only the duplex DNA ends (8, Figure 7B) but also the ssDNA/RNA strands threading through the central channel for stable binding. Consequently, human translin exhibits high binding affinity toward ssDNA and RNA as well as linear duplex DNA targets (8) (Figures 6A,C and 7), while *Drosophila* translin hardly binds either DNA or RNA sequences used in this study (Figure 6B). It is likely that the nonoctameric configuration associated with the *Drosophila* translin oligomer (Figure 5) might render its DNA/RNA binding belt in the concave part of the tetramer cup relatively ineffective, leading to loss in nucleic acid binding proficiency. Most surprisingly, we observed a decrease in human translin binding to all nucleic acid targets tested when GTP was added (Figure 7). The decrease was most prominent and specific to GTP in the case of the bona fide RNA target tested, namely, *Prm2* (Figure 7D). It appears that attenuation of ssDNA and dsDNA binding due to the GTP effect was somewhat marginal as compared to that with the RNA target (compare effects in panels A–C with that in panel D of Figure 7), which explains why earlier studies had missed the GTP effect on ssDNA binding (20). We believe that attenuation of DNA/RNA binding by translin in the presence of GTP is a manifestation of a structural dissociation, i.e., “loosening or slackening” in the ellipsoidal ring that lowers the nucleic acid tethering by the protein. Enhanced C-terminal cleavages by the protease action in the presence of GTP are a reflection of structural reorganization in the translin ring, and the lack of the same in *Drosophila* translin is consistent with the model that oligomeric status may be critical for the “switchability” by GTP. At this point, it is interesting to draw a parallel with well-characterized RAG1 and RAG2 proteins that perform critical DNA recognition and cleavage functions in V(D)J recombination, where physiological concentrations of GTP strongly and selectively inhibit the RAG-mediated transposition reaction (31). This encourages us to believe that GTP binding might similarly impinge on the proposed chromosomal breakage–rejoining function of translin, in vivo.

In summary, our results point out that GTP induces specific changes in human translin, which are largely absent in its *Drosophila* orthologue, and these effects are possibly related to their respective protein oligomeric states. Specific mutation studies might allow us to identify the motifs that would “humanize” *Drosophila* translin and will help to enhance our understanding of the complex relationship between protein oligomeric states and its function.

ACKNOWLEDGMENT

We gratefully acknowledge the help rendered by Rama Reddy, Nabanita Nag, and Dr. G. Krishnamoorthy of the Department of Chemical Sciences, TIFR, for the fluorescence studies. We are grateful to Murugan, B. T. Kansara, and Dr.

S. Mazumdar of the Department of Chemical Sciences, TIFR, for help with circular dichroism and ITC experiments. We thank Malini Natarajan, Ram Kumar Mishra, and Dr. Rohit Mittal of DBS, TIFR, for reagents and useful discussions. We also thank Dr. Vinay Kumar of BARC for critical comments on the experiments.

REFERENCES

- Aoki, K., Suzuki, K., Sugano, T., Tasaka, T., Nakahara, K., Kuge, O., Omori, A., and Kasai, M. (1995) A novel gene translin, encodes a recombination hotspot binding protein associated with chromosomal translocations, *Nat. Genet.* **10**, 167–174.
- Ishida, R., Okado, H., Sato, H., Shionoiri, C., Aoki, K., and Kasai, M. (2002) A role for the octameric ring protein, translin, in mitotic cell division, *FEBS Lett.* **525**, 105–110.
- Yang, S., Cho, Y. S., Chennathukuzhi, V. M., Underkoffler, L. A., Loomes, K., and Hecht, N. B. (2004) Translin-associated factor X is post-transcriptionally regulated by its partner protein TB-RBP, and both are essential for normal cell proliferation, *J. Biol. Chem.* **279**, 12605–12614.
- Han, J. R., Gu, W., and Hecht, N. B. (1995) Testis-brain RNA-binding protein, a testicular translational regulatory RNA-binding protein, is present in the brain and binds to the 3' untranslated regions of transported brain mRNAs, *Biol. Reprod.* **53**, 707–717.
- Wu, X. Q., Gu, W., Meng, X., and Hecht, N. B. (1997) The RNA-binding protein, TB-RBP, is the mouse homologue of translin, a recombination protein associated with chromosomal translocations, *Proc. Natl. Acad. Sci. U.S.A.* **94**, 5640–5645.
- Finkenstadt, P. M., Kang, W. S., Jeon, M., Taira, E., Tang, W., and Baraban, J. M. (2000) Somatodendritic localization of translin, a component of the translin/trax binding complex, *J. Neurochem.* **75**, 1754–1762.
- Kasai, M., Matsuzaki, T., Katayanagi, K., Omori, A., Maziarz, R. T., Strominger, J. L., Aoki, K., and Suzuki, K. (1997) The translin ring specifically recognizes DNA ends at recombination hot spots in the human genome, *J. Biol. Chem.* **272**, 11402–11407.
- Sengupta, K., and Rao, B. J. (2002) Translin binding to DNA: recruitment through DNA ends and the consequent conformational transitions, *Biochemistry* **41**, 15315–15326.
- Jacob, E., Puchshansky, L., Zeruya, E., Baran, N., and Manor, H. (2004) The human protein translin specifically binds single-stranded microsatellite repeats, d(GT)_n, and G-strand telomeric repeats, d(TTAGGG)_n: a study of the binding parameters, *J. Mol. Biol.* **344**, 939–950.
- Kaluzhny, D., Laufman, O., Timofeev, E., Borisova, O., Manor, H., and Shchyolkina, A. (2005) Conformational changes induced in the human protein translin and in the single-stranded oligodeoxynucleotides d(GT)₁₂ and d(TTAGGG)₅ upon binding of these oligodeoxynucleotides by translin, *J. Biomol. Struct. Dyn.* **23**, 257–265.
- Wang, J., Boja, E. S., Oubrahim, H., and Chock, P. B. (2004) Testis brain ribonucleic acid-binding protein/translin possesses both single-stranded and double-stranded ribonuclease activities, *Biochemistry* **43**, 13424–13431.
- Aoki, K., Ishida, R., and Kasai, M. (1997) Isolation and characterization of a cDNA encoding a translin-like protein, *FEBS Lett.* **401**, 109–112.
- Gupta, G. D., Makde, R. D., Kamdar, R. P., D'Souza, J. S., Kulkarni, M. G., Kumar, V., and Rao, B. J. (2005) Co-expressed recombinant human translin-trax complex bind DNA, *FEBS Lett.* **579**, 3141–3146.
- Chennathukuzhi, V. M., Kurihara, Y., Bray, J. D., and Hecht, N. B. (2001) TRAX (translin associated factor X), a primarily cytoplasmic protein inhibits the binding of TB-RBP (translin) to RNA, *J. Biol. Chem.* **276**, 13256–13263.
- Sengupta, K., Suseendranathan, K., Rikhy, R., D'Souza J. S., Kokkanti, M., Kamdar, R., Singh, K., Subramanian, L., Rodrigues, V., and Rao, B. J. GenBank accession number AY392453 (unpublished data).
- Bourne, H. R., Sanders, D. A., and McCormick, F. (1990) The GTPase superfamily: a conserved switch for diverse cell functions, *Nature* **348**, 125–132.
- Bourne, H. R., Sanders, D. A., and McCormick, F. (1991) The GTPase superfamily: conserved structure and molecular mechanism, *Nature* **349**, 117–127.
- Takai, Y., Sasaki, T., and Matozaki, T. (2001) Small GTP-binding proteins, *Physiol. Rev.* **81**, 153–208.
- Sprang, S. R. (1997) G protein mechanisms: insights from structural analysis, *Annu. Rev. Biochem.* **66**, 639–678.
- Chennathukuzhi, V. M., Kurihara, Y., Bray, J. D., Yang, J., and Hecht, N. B. (2001) Altering the GTP binding site of the DNA/RNA-binding protein, translin/TB-RBP, decreases RNA binding and may create a dominant negative phenotype, *Nucleic Acids Res.* **29**, 4433–4440.
- Pascal, J. M., Chennathukuzhi, V. M., Hecht, N. B., and Robertus, J. D. (2002) Crystal structure of TB-RBP, a novel RNA-binding and regulating protein, *J. Mol. Biol.* **319**, 1049–1057.
- Wiseman, T., Williston, S., Brandts, J. F., and Lin, L. N. (1989) Rapid measurement of binding constants and heats of binding using a new titration calorimeter, *Anal. Biochem.* **79**, 131–137.
- Mustafi, S. M., Mukherjee, S., Chary, K. V. R., Vianco, C. D., and Luchinat, C. (2004) Energetics and mechanism of Ca²⁺ displacement by lanthanides in a calcium binding protein, *Biochemistry* **43**, 9320–9331.
- Wu, X.-Q., and Hecht, N. B. (2000) Mouse testis brain ribonucleic acid-binding protein/translin colocalizes with microtubules and is immunoprecipitated with messenger ribonucleic acids encoding myelin basic protein, α calmodulin kinase II, and protamines 1 and 2, *Biol. Reprod.* **62**, 720–725.
- Sugiura, I., Sasaki, C., Hasegawa, T., Kohno, T., Sugio, S., Moriyama, H., Kasai, M., and Matsuzaki, T. (2004) Structure of human translin at 2.2 Å resolution, *Acta Crystallogr., Sect. D: Biol. Crystallogr.* **60**, 674–679.
- Vanlooock, M. S., Chen, Y. J., Yu, X., Patel, S. S., and Egelman, E. H. (2001) Electron microscopic studies of the translin octameric ring, *J. Struct. Biol.* **135**, 58–66.
- Aoki, K., Suzuki, K., Ishida, R., and Kasai, M. (1999) The DNA binding activity of translin is mediated by a basic region in the ring-shaped structure conserved in evolution, *FEBS Lett.* **443**, 363–366.
- Holley, R. W., Apgar, J. W., Doctor, B. P., Farrow, J., Marini, M. A., and Merrill, S. H. (1961) A simplified procedure for the preparation of tyrosine- and valine-acceptor fractions of yeast "soluble ribonucleic acid", *J. Biol. Chem.* **236**, 200–202.
- Castro, A., Peter, M., Magnaghi-Jaulin, L., Vigneron, S., Loyaux, D., Lorca, T., and Labbe, J.-C. (2000) Part of *Xenopus* translin is localized in the centrosomes during mitosis, *Biochem. Biophys. Res. Commun.* **276**, 515–523.
- Laufman, O., Yosef, B. R., Adir, N., and Manor, H. (2005) Cloning and characterization of the *Schizosaccharomyces pombe* homologs of the human protein translin and the translin-associated protein TRAX, *Nucleic Acids Res.* **33**, 4128–4139.
- Tsai, C. L., and Schatz, D. G. (2003) Regulation of RAG1/RAG2-mediated transposition by GTP and the C-terminal region of RAG2, *EMBO J.* **22**, 1922–1930.

BI050540E